

Analysis of self-similar solution of the advection dominated flows around a black hole

J.R. Bhatt and A.R. Prasanna

Physical Research Laboratory, Navarangpura, Ahmedabad 380 009, India (jeet.prasanna@prl.ernet.in)

Received 17 December 1999 / Accepted 5 April 2000

Abstract. We analyze self-similar solution of advection dominated accretion flows around a black-hole. The effect of a pseudo-Newtonian potential is introduced perturbatively, i.e., by regarding the general relativistic effects to be small. Comparison is made with the exact global numerical solutions that exist in the literature. It is demonstrated that the perturbative analysis can give better representation and insight into the parameter space of the solution. We find over a large range of the viscosity parameter, that self-similarity could be an excellent approximation. However, for certain values of the viscosity parameter and the gas parameter γ , the perturbation can have a singularity. Consequently, the assumption of self-similarity could be violated at distances far away from the central black hole. Implication of the perturbative analysis is discussed.

Key words: hydrodynamics – black hole physics – accretion, accretion disks

1. Introduction

As suggested by the recent studies a class of accretion disk models invoking advection have been successful in explaining low luminosity accreting black hole systems (see Narayan et al. 1998 for a review). In these models viscously generated internal energy is not radiated out immediately – as in the standard thin disk model – but stored in the accreting gas. The stored energy might eventually be lost into the black hole or a considerable portion of it might give rise to wind (Blandford & Begelman 1999). This kind of accretion flows, when there is no out flow, are known as advection dominated accretion flows (ADAFs). By definition ADAFs have very low radiative efficiency and as a consequence they can be considerably hotter than the gas flow in the standard disk models (Narayan & Yi 1995a,b).

ADAFs can occur in two distinct physical regimes. Firstly they can occur when the accreting gas density and consequently its optical depth become higher due to very high mass accretion rates (in super-Eddington limit) (Begelman 1978; Begelman & Meier 1982). In this limit radiation can be trapped in the in-falling gas. Accretion flow in this case was found to be stable against thermal and viscous instabilities (Abramowicz et al.

1988, Kato et al. 1996). Secondly, ADAFs can occur when the infalling gas has low density and low optical depth when the mass accretion rates become very small (Ichimaru 1977, Rees et al. 1982, Narayan & Yi 1994, 1995a,b, Abramowicz et al. 1995, Chen 1995). In this limit radiative time scale becomes lower than the accretion time scale and as a result almost all the internal energy can be lost to the black hole.

Models of optically thin branch of ADAFs comprising two-temperature plasma have recently found many promising applications in explaining various low luminosity accreting black hole systems. Advection models for Sagittarius A* at the center of our galaxy (Rees et al. 1982, Narayan et al. 1995), and for NGC 4258 (Lasota et al. 1996) have been proposed. It has also been suggested that the center of many elliptical galaxies might be accreting in advection dominated mode (Fabian & Rees 1995, Mahadevan 1997). Moreover, ADAF models have been applied to X-ray transients A0620 -00, V404 Cyg and Nova Muscae 1991 in their quiescent states (Narayan et al. 1996). It must be noted that all the above models were based on local self-similar solution of ADAFs (Narayan & Yi 1994, Spruit et al. 1987).

The local self-similar solutions are generally assumed to be valid in the region away from the boundaries. But in their application in spectral calculations their validity is assumed right up to the last marginally stable orbit. It ought to be noted that the self-similar solution does not have a trans-sonic region. However, in realistic situation the radial flow velocity could approach that of light in the vicinity of the black-hole. Due to inefficient radiative processes sound velocity can also increase but the radial velocity can over take it. In other words one might expect trans-sonic region and sonic point in the accretion flows. Keeping this limitation in mind, perhaps, study of global solution of optically thin branch of the ADAFs had been started. First the global solutions were found for a pseudo-Newtonian potential (Narayan et al. 1997 (NKH), Chen et al. 1997) and later for a full Kerr metric (Abramowicz et al. 1996, Peitz & Appl 1997, Gammie & Popham 1998). In the above, exact numerical studies, it was found that the self-similar solutions are good approximations in the region outside the sonic point.

It ought to be noted that the self-similar solution to optically thin branch of ADAFs (Narayan & Yi 1994, Spruit et al. 1987) was found using the Newtonian potential. But the symmetry leading to self-similarity can be destroyed if any non-Newtonian

form of the potential is used. The self-similarity can also be destroyed if the specific angular momentum per unit mass accreted by the black hole j is comparable or larger than ΩR^2 . Here, ΩR is azimuthal velocity of the accreting gas and R is the radial coordinate. In what follows we assume $\Omega R^2 \gg j$. Exact numerical solutions of Gammie & Popham 1998 shows that this assumption is justified. However for the case of thin accretion disk this can not be ascertained. We check this assumption for the case of approximate solution in Appendix -A.

Taking the above facts into consideration, we adopt an alternative approach to study the validity of the self similar solution. We regard the self-similar solution as a ‘background’ and introduce effect of pseudo-Newtonian potential in a perturbative fashion. At the distances very far from the central object the perturbations due to the non-Newtonian potential can be extremely small, but as one moves closer to the center they can grow. Of course, with this technique one can not go arbitrarily close to the central object, as the underlying assumption of the perturbation theory may break down. However, if the perturbations can grow and become comparable to the background much before the event horizon is reached, then the point where the perturbation breaks down can be regarded as the point up to which the self-similar solution has its validity. Therefore, this approach can give us a more accurate criterion for the validity of the self similar solution. This method can also provide an appropriate parameter space where the assumption of self-similarity is valid. These features are difficult to be seen in the earlier exact but numerical approach to the global solutions. Therefore, we believe that the present work should be considered to be complimentary to the earlier work on the global solutions.

In Sect. 2 we write the basic set of differential equations for the perturbation theory. Sect. 3 discusses self-similar solutions and the results from perturbation theory. Finally we compare our results with the exact numerical global solutions obtained by NKH. Also the relevance of the perturbation theory results to the earlier work is discussed.

2. Basic equations

Recently it was demonstrated by Narayan & Yi (1995a) that the steady state self-similar regime of advection dominated accretion flows operates in the region far off the boundaries. Therefore height-integrated set of fluid equations can well describe the accretion flow at least in the self-similar regime. Later it was shown by NKH that correction introduced by the non-sphericity remains under control even when the effect of boundary near the sonic point is considered. We consider height-integrated set of equations describing steady state axisymmetric equations (see NKH and references cited therein). In steady state and axisymmetry, the height-integrated hydrodynamical equations allow one to describe all the physical quantities as function of the cylindrical radius R only. Within these approximations the mass continuity equation takes form

$$\frac{d}{dR} (2\pi \cdot R \cdot 2H \cdot \rho v) = 0 \quad (1)$$

where ρ is the density of the gas, H is the vertical ‘‘half-thickness’’, and v is the radial velocity. Eq. (1) can be readily integrated to give mass accretion rate,

$$-4\pi R H \rho v = \dot{M} = \text{constant} \quad (2)$$

where H is defined in terms of isothermal sound speed as

$$H = \left(\frac{5}{2}\right)^{1/2} \frac{c_s}{\Omega_k} \quad (3)$$

where Ω_k is the Keplerian angular velocity. Factor $(5/2)^{1/2}$ is chosen in the same way as NKH i.e. in order to obtain correct result for spherical flow $\dot{M} = -4\pi R^2 \rho v$.

We assume that the gravitational potential of the central black-hole is described by the pseudo-Newtonian potential (Paczynski & Wiita 1980)

$$\Phi = -\frac{GM}{R - R_g} \quad (4)$$

where M is the mass of the black hole and $R_g = \frac{2GM}{c^2}$ is the gravitational radius. This would allow us to define the Keplerian angular velocity Ω_{kn} in the pseudo-Newtonian potential as

$$\Omega_{kn}^2 = \frac{GM}{R(R - R_g)^2} \quad (5)$$

It should be noted that we use Ω_{kn} in place of Ω_k in Eq. (3) in what follows as in the earlier work by Chen et al. (1997) and NKH. Radial momentum equation of the accreting gas is given by

$$v \frac{dv}{dR} = -\Omega_{kn}^2 R + \Omega^2 R - \frac{1}{\rho} \frac{dp}{dR} \quad (6)$$

where Ω is the angular velocity of the gas. The pressure p can be written in terms of isothermal sound speed as

$$p = \rho c_s^2 \quad (7)$$

The steady state angular momentum equation in the presence of viscosity can be written as

$$v \frac{d}{dR} (\Omega R^2) = \frac{1}{\rho R H} \frac{d}{dR} \left(\nu \rho R^3 H \frac{d\Omega}{dR} \right) \quad (8)$$

where $\nu = \alpha \frac{c_s^2}{\Omega_{kn}}$ is the kinematic viscosity. Here α is assumed to be independent of R . Using Eq. (2) one can integrate the equation for the angular momentum to obtain

$$\frac{d\Omega}{dR} = \frac{v \Omega_{kn} (\Omega R^2 - j)}{\alpha R^2 c_s^2} \quad (9)$$

The integration constant j represent angular momentum per unit mass accreted by the black hole and it is to be determined self-consistently as an eigen-value problem. However, it ought to be noted that the self-similar solution does satisfy Eq. (9) only when $j \leq \Omega R^2$.

Finally we consider the energy balance between the local viscous heating and local radiative cooling giving rise to overall heat transport (advection). We write this as an entropy equation. The entropy rate is determined by the local viscous heating rate minus local cooling rate. However, in the case when advection dominates the cooling rate is negligible compared to the viscous heating rate. But for generality we retain the cooling term and write it as factor $(1 - f)$ times the heating rate term. The energy equation can then be written as

$$\frac{\rho v}{(\gamma - 1)} \frac{dc_s^2}{dR} - c_s^2 v \frac{d\rho}{dR} = \frac{f \alpha \rho c_s^2 R^2}{\Omega_{kn}} \left(\frac{d\Omega}{dR} \right)^2 \quad (10)$$

where γ is the ratio of specific heats of the accreting gas. f is in general a function of R , but for an advection dominated flow $f(R) \sim 1$ i.e. constant. However, $f(R) \ll 1$ for the cooling dominated flow.

One of the aims of this paper is to incorporate the effect of pseudo-Newtonian gravitational potential perturbatively and thereby increase the accuracy of the self-similar solution. Therefore, we first briefly review the self-similar solutions (Narayan & Yi 1994). Self-similar solution of Eqs. (1–10) was obtained by setting $\frac{R_g}{R} = 0$ in Eq. (4) and $\Omega_{kn} \rightarrow \Omega_k$, where Ω_k is the Keplerian angular velocity in the presence of Newtonian gravitational potential. Expressions for the radial velocity v , sound speed c_s , angular velocity Ω and density ρ in this limit are given by

$$v = v_0 \left(\frac{R}{R_g} \right)^{-1/2} \quad (11)$$

$$c_s = c_{s0} \left(\frac{R}{R_g} \right)^{-1/2} \quad (12)$$

$$\Omega = \Omega_0 \left(\frac{R}{R_g} \right)^{-3/2} \quad (13)$$

$$\rho = \rho_0 \left(\frac{R}{R_g} \right)^{-3/2} \quad (14)$$

where the dimensional constants v_0, c_{s0}, Ω_0 and ρ_0 are defined as

$$v_0 = -\frac{(5 + 2\epsilon) g}{3\alpha} \frac{c}{\sqrt{2}} \quad (15)$$

$$c_{s0} = \left[\frac{(5 + 2\epsilon) g}{9\alpha^2} \right]^{1/2} c \quad (16)$$

$$\Omega_0 = \left[\frac{\epsilon(5 + 2\epsilon) g}{9\alpha^2} \right]^{1/2} \frac{c}{R_g} \quad (17)$$

$$\rho_0 = \frac{9\alpha^2 \dot{M} R_g^{-2}}{4\pi \sqrt{5/2} [(5 + 2\epsilon) g]^{3/2} c} \quad (18)$$

where, c is the speed of light, $\epsilon = \left(\frac{1}{f} \right)^{\frac{5}{3}} - \frac{g}{g - 1}$ and $g =$

$$\sqrt{1 + \frac{18\alpha^2}{(5 + 2\epsilon)^2}} - 1. \text{ If we substitute for } v_0, c_{s0}, \Omega_0 \text{ and } \rho_0$$

from Eqs. (15–18) into Eqs. (11–14) and use the definition of R_g one can obtain the self-similar solution of Narayan & Yi (1994).

In order to study how the effects of non-Newtonian potential can affect the self-similar solution in the region far from R_g , we introduce perturbation in the hydrodynamical quantities as $v \rightarrow v + \delta v, c_s \rightarrow c_s + \delta c_s, \Omega \rightarrow \Omega + \delta \Omega$ and $\rho \rightarrow \rho + \delta \rho$. Here, the ‘background’ quantities v, c_s, Ω and ρ describe the self-similar solutions in Eqs. (11–14) and which can satisfy the height integrated hydrodynamical Eqs. (1–10) when $\frac{R_g}{R}$ is negligible. The quantities like δA represent the perturbation introduced by the pseudo-Newtonian potential.

Next, we consider the perturbations in Keplerian velocity due to pseudo-Newtonian gravitational potential. From Eq. (5), when $R > R_g$, one can write

$$\Omega_{kn}^2 \simeq \frac{GM}{R^3 \left(1 - 2\frac{R_g}{R} \right)} \simeq \Omega_k^2 + 2 \left(\frac{R_g}{R} \right) \Omega_k^2 \quad (19)$$

where $\Omega_k^2 = \frac{GM}{R^3}$. And Ω_{kn} can be written from Eq. (19) as

$$\Omega_{kn} \simeq \Omega_k + \left(\frac{R_g}{R} \right) \Omega_k \quad (20)$$

In writing Eqs. (19–20) we have neglected the terms of the order $\left(\frac{R_g}{R} \right)^2$ and higher. From the above we have $\delta \Omega_{kn}^2 = 2 \left(\frac{R_g}{R} \right) \Omega_k^2$ and $\delta \Omega_{kn} = \left(\frac{R_g}{R} \right) \Omega_k$.

We linearize the Eqs. (2, 3, 6, 7, 9–10) and retain the terms which are first order in perturbed quantities and $O \left(\frac{R_g}{R} \right)$,

$$\frac{\delta H}{H} + \frac{\delta \rho}{\rho} + \frac{\delta v}{v} = 0 \quad (21)$$

$$\frac{\delta H}{H} = \frac{\delta c_s}{c_s} - \frac{R_g}{R} \quad (22)$$

$$v \frac{d\delta v}{dR} + \delta v = -2 \left(\frac{R_g}{R} \right) \Omega_k^2 R + 2\Omega \delta \Omega R + \frac{\delta \rho}{\rho^2} \frac{d\rho}{dR} - \frac{1}{\rho} \frac{d\delta \rho}{dR} \quad (23)$$

$$\delta p = \delta \rho c_s^2 + 2\rho c_s \delta c_s \quad (24)$$

$$\begin{aligned} \alpha c_s^2 \left(\frac{d\Omega}{dR} \right) \left[2 \frac{\delta c_s}{c_s} + \left(\frac{d\Omega}{dR} \right)^{-1} \frac{d\delta \Omega}{dR} \right] \\ = v \Omega_k \Omega \left[\frac{\delta v}{v} + \frac{R}{R_g} + \frac{\delta \Omega}{\Omega} \right] \end{aligned} \quad (25)$$

$$\frac{\rho v}{(\gamma - 1)} \frac{dc_s^2}{dR} \left[\frac{\delta \rho}{\rho} + \frac{\delta v}{v} + 2 \left(\frac{dc_s^2}{dR} \right)^{-1} \frac{d(2c_s \delta c_s)}{dR} \right]$$

$$\begin{aligned}
& -c_s^2 v \frac{d\rho}{dR} \left[2 \frac{\delta c_s}{c_s} + \frac{\delta v}{v} + \left(\frac{d\rho}{dR} \right)^{-1} \frac{\delta \rho}{\rho} \right] \\
& = \frac{f \alpha R^2 \rho c_s^2}{\Omega_k} \left(\frac{d\Omega}{dR} \right)^2 \left[\frac{\delta \rho}{\rho} + 2 \frac{\delta c_s}{c_s} - \frac{R_g}{R} + 2 \frac{\delta \Omega}{\Omega} \right] \quad (26)
\end{aligned}$$

It should be noted that in writing Eq. (25) we have assumed $\delta \Omega R^2 > j$ as in the background self-similar solution of Narayan & Yi (1994). Eqs. (21–26) have inhomogeneous terms introduced by the perturbations in the gravitational potential. In the spirit of the self-similar solution, we look for the solution in powers of R for the perturbation equations. It can also be noticed that in order to satisfy Eq. (23) all the terms containing perturbed quantities must have radial dependence like R^{-3} . This can dictate following choice for the perturbations:

$$\delta v = v_{01} \left(\frac{R_g}{R} \right)^{3/2} \quad (27)$$

$$\delta c_s = c_{s01} \left(\frac{R_g}{R} \right)^{3/2} \quad (28)$$

$$\delta \Omega = \Omega_{01} \left(\frac{R_g}{R} \right)^{5/2} \quad (29)$$

$$\delta \rho = \rho_{01} \left(\frac{R_g}{R} \right)^{5/2} \quad (30)$$

where v_{01} , c_{s01} , Ω_{01} and ρ_{01} are unknown dimensional constants and have dimensions of velocity, angular velocity and density as suggested from their standard notations. These constants are yet to be determined (below).

It can be seen from Eqs. (11–14, 27–30):

$$\begin{aligned}
\frac{\delta v}{v} &= \frac{v_{01}}{v_0} \left(\frac{R_g}{R} \right), \\
\frac{\delta c_s}{c_s} &= \frac{c_{s01}}{c_{s0}} \left(\frac{R_g}{R} \right) \quad \frac{\delta \Omega}{\Omega} = \frac{\Omega_{01}}{\Omega_0} \left(\frac{R_g}{R} \right)
\end{aligned}$$

Thus all the perturbed quantities are well behaved functions of radial coordinate R over the entire region of interest *i.e.* $R_g < R < \infty$. However, one cannot still ascertain that the perturbations are small over the above range of R . This is because of the fact that quantities like $\frac{v_{01}}{v_0}$, $\frac{c_{s01}}{c_{s0}}$ etc. are functions of α , ϵl , γ and they can, in general, have values larger than unity. One can regard the perturbation theory to be valid till the magnitude of the perturbed quantity is less than that of the corresponding background quantity. From this one can have a criterion for the validity of the perturbation as $R_p(v) = |v_{01}/v_0|$. Here R_p is the radius beyond which the perturbation theory is valid. Thus for $R < R_p(v)$ perturbation of the radial velocity becomes larger than the background and therefore perturbed solution of v should be discarded. It should be noted that each quantity has different region of validity for the perturbation.

If we substitute for all the perturbed quantities in Eqs. (21, 23, 25–26) from Eqs. (27–30) one can check in a straightforward algebra that the radial dependence can be factored out if the

explicit form of the self-similar solution is substituted. We can write equations for the unknown coefficients of the perturbed quantities as:

$$\begin{aligned}
& \left[\frac{(5+2\epsilon l)g}{9\alpha^2} - \frac{(5+2\epsilon l)^2 g^2}{9\alpha^2} \right] \left(\frac{v_{01}}{v_0} \right) \\
& - \frac{2\epsilon l(5+2\epsilon l)g}{9\alpha^2} \left(\frac{\Omega_{01}}{\Omega_0} \right) - 6 \left[\frac{(5+2\epsilon l)g}{9\alpha^2} \right] \left(\frac{c_{s01}}{c_{s0}} \right) \\
& = -1 + \left\{ \frac{(5+2\epsilon l)g}{9\alpha^2} \right\} \quad (31)
\end{aligned}$$

$$-\frac{3}{2} \left(\frac{v_{01}}{v_0} \right) + \frac{\Omega_{01}}{\Omega_0} + 3 \left(\frac{c_{s01}}{c_{s0}} \right) = \frac{3}{2} \quad (32)$$

$$\begin{aligned}
& (\gamma-1) \left(\frac{v_{01}}{v_0} \right) + (5/3-\gamma) \left(\frac{\Omega_{01}}{\Omega_0} \right) \\
& - 2(\gamma+1) \left(\frac{c_{s01}}{c_{s0}} \right) = 7 - 5\gamma \quad (33)
\end{aligned}$$

In order to determine the unknown coefficients of the perturbations we need to solve the set of simultaneous Eqs. (31–33). The solution can be found in a rather straight forward way and it can be written as

$$\begin{aligned}
\frac{c_{s01}}{c_{s0}} &= \left\{ (19-13\gamma)9\alpha^2 + (11-5\gamma)f1^2 \right. \\
& \left. - 6f1[3(5/3-\gamma) + 4\epsilon l(1-\gamma)] \right\} / \left\{ 4f1(12\epsilon l \right. \\
& \left. + 15-13\gamma) + (54-26\gamma)f1^2 \right\} \quad (34)
\end{aligned}$$

where, $f1 = (5+2\epsilon l)g$. Perturbation coefficient of all other quantities can be written in terms of $\frac{c_{s01}}{c_{s0}}$ as

$$\frac{v_{01}}{v_0} = -\frac{11-5\gamma}{19-13\gamma} + \frac{54-26\gamma}{19-13\gamma} \left(\frac{c_{s01}}{c_{s0}} \right) \quad (35)$$

$$\frac{\Omega_{01}}{\Omega_0} = 12 \left(\frac{1-\gamma}{19-13\gamma} \right) + \frac{27}{19-13\gamma} \left(\frac{c_{s01}}{c_{s0}} \right) \quad (36)$$

The coefficient of density perturbation can be found, using Eqs. (21–22), as

$$\frac{\rho_{01}}{\rho_0} = 1 - \frac{v_{01}}{v_0} - \frac{c_{s01}}{c_{s0}} \quad (37)$$

3. Discussion and summary

Thus, we have obtained the following corrections of the order of $O(R_g/R)$ due to the pseudo-Newtonian potential over the self-similar solution of Narayan & Yi 1994;

$$\rho = \rho_0 \left(\frac{R_g}{R} \right)^{3/2} \left[1 + \frac{\rho_{01}}{\rho} \left(\frac{R_g}{R} \right) \right] \quad (38)$$

$$v = v_0 \left(\frac{R_g}{R} \right)^{1/2} \left[1 + \frac{v_{01}}{v_0} \left(\frac{R_g}{R} \right) \right] \quad (39)$$

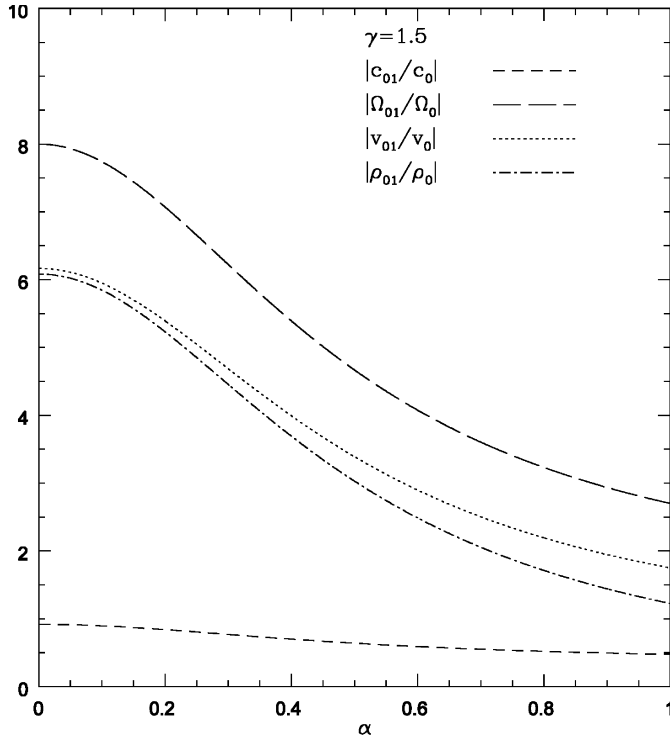


Fig. 1. Ratios of magnitude of the coefficients of perturbed quantities to the coefficients of self-similar solution are plotted, for $\gamma = 1.5$, as functions of α . The plot indicates all the ratios: velocity $|v_{01}/v_0|$, sound speed $|c_{01}/c_0|$, angular frequency $|\Omega_{01}/\Omega_0|$ and density $|\rho_{01}/\rho_0|$ are well behaved functions of α .

$$c_s = c_{s0} \left(\frac{R_g}{R} \right)^{1/2} \left[1 + \frac{c_{s01}}{c_0} \left(\frac{R_g}{R} \right) \right] \quad (40)$$

$$\Omega = \Omega_0 \left(\frac{R_g}{R} \right)^{3/2} \left[1 + \frac{\Omega_{01}}{\Omega_0} \left(\frac{R_g}{R} \right) \right] \quad (41)$$

where, all the coefficients with the suffix '0' can be determined from Eqs. (15–18) and they are exactly the same as self-similar solutions of Narayan & Yi (1994), while the perturbation coefficients $\frac{A_{01}}{A_0}$; $A = c_s, v, \Omega, \text{ or } \rho$ can be determined from Eqs. (34–37).

Using Eqs. (34–37) we can study the magnitude of the perturbed quantities as functions of α and γ . In Figs. 1–2 we plot ratios of the coefficients of perturbation to the coefficients of self-similar solution: $|v_{01}/v_0|$, $|c_{s01}/c_{s0}|$, $|\Omega_{01}/\Omega_0|$ and $|\rho_{01}/\rho_0|$ as functions of α .

Fig. 1 shows the behaviour of perturbed parameters for the case $\gamma=1.5$. Four curves of all the perturbed quantities mentioned above are shown for the entire range of the viscosity parameter α i.e. $0 < \alpha \leq 1$. Magnitude of the coefficient of perturbation in sound velocity remain less than unity over the complete range of α . This in turn implies that $\frac{c_{s01}}{c_{s0}}$ remains finite over the entire range $R_g < R < \infty$. Thus self-similarity is an excellent approximation for sound speed in ADAF. This feature had been first observed by NKH. Magnitude of the velocity perturbation remains greater than unity for all values of

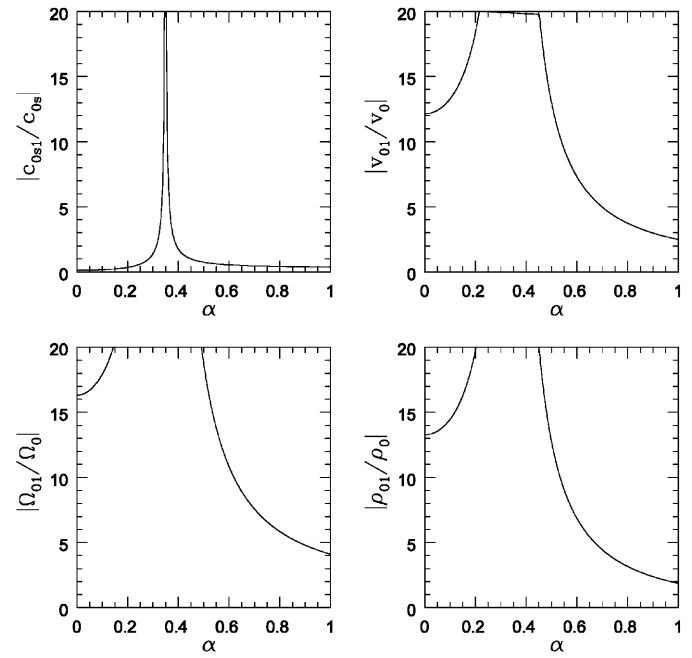


Fig. 2. Caption is same as Fig. 1 but the case is shown for $\gamma=1.55$. The plot indicates a singularity in the ratio around $\alpha \simeq 0.35$. This indicates a complete breakdown of the self-similarity over a very large distances from the central compact object.

the viscosity parameter. However, $|v_{01}/v_0|$ decreases with increasing values of α . From the above discussed validity criterion of the perturbation, one can see that for lower values of $\alpha (\ll 1)$, the perturbation grows faster as compared to case where $\alpha \simeq 1$. In other words it seems that self-similarity is a good approximation for velocity perturbation in the proximity of the central object only for the higher values of α . Similar trends can be seen in $|\Omega_{01}/\Omega_0|$ and $|\rho_{01}/\rho_0|$ i.e. the perturbations are strongest in $\alpha \rightarrow 0$ limit. In this regime the strongest departure from self-similarity can occur when $R \leq 8R_g$ for $|\Omega_{01}/\Omega_0|$ and $R \leq 6R_g$ for $|\rho_{01}/\rho_0|$.

All the above features reported for $\gamma = 1.5$ case in Fig. 1 are broadly in agreement with the global solutions of ADAFs obtained by NKH. In other words, our perturbative analysis confirms their results: (a) self-similar behavior of the sound velocity, in the presence of pseudo-Newtonian potential, remains more accurate compared to those for the radial velocity, angular velocity and density. (b) self-similarity violations are stronger in the low α regime. However, it must be noted that our analysis does not treat the inner boundary incorporating $j \neq 0$, and therefore one cannot confirm the prediction of the sonic point.

For $\gamma = 1.55$ all the above perturbed quantities can be plotted as functions of α . However, for some values of α we find that the magnitude of the perturbations grows indefinitely, although both on higher and on lower side of this critical α_c value, the perturbations have controlled behavior. Top left panel in Fig. 2 depicts logarithm of the ratio of the coefficient of sound perturbation to that of the self-similar sound velocity as a function of α . It shows that the perturbation can grow indefinitely around $\alpha \simeq 0.35$. All the other perturbed quantities have the similar be-

havior around the same value of α , as shown in the figure. Also there is an over all increase in values of all perturbed quantities in the regions $\alpha \ll \alpha_c$ and $\alpha > \alpha_c$ as compared to Fig. 1. This may be indicative of high sensitivity of the solution depending on γ .

In view of the above, a natural question is, whether the singular behavior is only an artifact of the perturbative approach or it is genuine? In what follows we try to answer this question.

Presence of the gravity term in Eq. (6) can introduce inhomogeneity, which can dictate the form of any power solution. In the present case, inhomogeneous term would read $-\Omega_{kn}^2 R = -(GM/R^2) [1 + 2R_g/R + 3(R_g/R)^2 \dots]$. It is the first term on the right hand side which gives the self-similar solution as zeroth order in the expansion. In general the solution for the n th order can have the following form ($n = 0, 1, 2, 3, \dots$): v_n, c_{sn} go like $(R_g/R)^{(2n+1)/2}$ and Ω_n, ρ_n go like $(R_g/R)^{(2n+3)/2}$. Since $R_g/R \ll 1$ we can ascertain that all the higher orders in perturbations are smaller than their counter parts in the lower order. Therefore, the singularity in the parameter space should be considered to be genuine. Moreover, the singularity should manifest itself in the global numerical solutions also. It appears that the system does indicate a strange behavior for higher α at $\gamma = 1.55$. In fact it has been noticed by others too, that the numerical global solution code seem to develop difficulties in integration, for the value $\gamma = 1.55$ and higher α (Narayan 1999, Private communication).

This in turn would imply that the breakdown of the perturbation analysis and the problem faced in numerical integration could be indicative of a new branch of solution. Whether the new branch of solution is related with the shock singularity (Chakrabarti 1996, Chakrabarti & Titarchuk 1995) can not be answered within the framework of the perturbative approach. However, the breakdown of the self-similarity, in the present work, occurs in a rather small region of the parameter space unlike the referred work of Chakrabarti & Titarchuk (1995).

Finally we compare our perturbative solution with the global solution of NKH and the self-similar solution. In Fig. 3 we plot radial velocity v , sound speed c_s and angular frequency Ω as function of R/R_g for $\alpha=0.3$ and $\gamma=1.5$. In general our perturbative solution (SP) provides a better approximation to the exact global solution (NKH) as compared to the self-similar solution (SS) especially for the region R/R_g small. It also reconfirms that the self-similar profile of sound velocity is a good approximation even at the smaller values of R/R_g for the current values of α and γ .

In summary, we have studied the self-similar solution in a pseudo-Newtonian potential in a perturbative fashion. We have also shown that our approximate solution provide a better approximation to the exact global but numerical solution in proximity of the central object. We find that our approach gives a convenient representation of the parameter space of the self-similar solutions. It is also shown that for $\gamma = 1.55$, the self-similarity would be broken in the region far away from the central compact object.

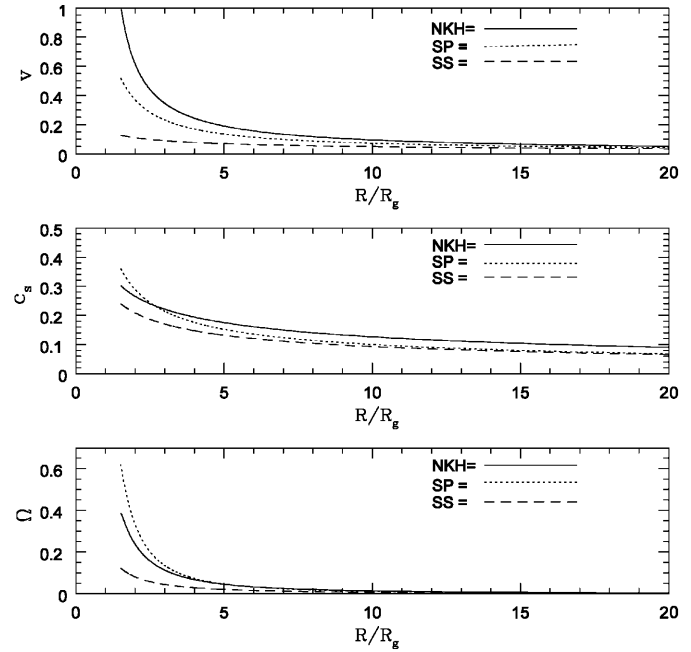


Fig. 3. Curves with solid lines show exact global numerical solution of NKH (see text), while the curves with dotted lines show our approximate solution (SP). The dashed curve represent self-similar (SS) solution of Narayan & Yi 1995a. All the results are obtained for $\alpha=0.3$ and $\gamma=1.5$. *Top:* variation of radial velocity with the radius. *Middle:* variation of sound velocity. *Bottom:* shows variation of angular frequency with radius. The plot shows that the perturbative solution provides a better approximation to the global solution at small radii.

Acknowledgements. It is a pleasure to thank Ramesh Narayan for many useful discussion at the various stages of this work and for providing us the numerical code for the global solution. One of us (J.R.B) would like to thank E. Quataert for some useful tips in handling the code. We would like to thank the referee of this paper for providing very useful criticism which has helped us in improving our presentation.

Appendix A

We can now compare the effect of non-Newtonian potential with the finite specific angular momentum constant j . Values of j should be determined from an eigen-value problem (e.g. Chen et al. 1997 determine $j = 0.9$ in the unit of Keplerian angular momentum at $3R_g$ for $\alpha=0.1$). Typically values of j ranges from 0.4 to 1.0 in the above mentioned units. Exact numerical calculations of Gammie & Popham 1998 (see Fig. 1) indicates that this is indeed true. Moreover, one can estimate that this is the case from the approximate solutions as follows:

Consider

$$\Omega R^2 - j = \left[\frac{\Omega}{\Omega(3R_g)} \left(\frac{R}{R_g} \right)^2 - \frac{j}{j(3R_g)} \right] j(3R_g).$$

Next, we use Eq. (29) to substitute for Ω

$$\Omega R^2 - j = \left[\sqrt{24} \left(\frac{\epsilon l (2 + 5\epsilon l)}{9\alpha^2} \right)^{1/2} \left(\frac{R}{R_g} \right)^{1/2} - 0.9 \right] \times j(3R_g)$$

If we take $\alpha = 0.1$, $f \simeq 1$ and $\gamma = 1.5$, $\epsilon' \simeq 0.33$ and thus one can have $\Omega R^2 \simeq \left[18 (R/R_g)^{1/2} - 0.9\right]$. Since $R > R_g$, our assumption $\Omega R^2 \gg j$ is justified.

References

- Abramowicz M.A., Czerny B., Lasota J.-P., Szuszkiewicz E. 1988, ApJ 332, 646
- Abramowicz M.A., Chen X., Kato S., et al., 1995, ApJ 483, L37
- Abramowicz M.A., Chen X., Granath M., Lasota J.-P., 1996, ApJ 471, 762
- Begelman M., 1978, MNRAS 184, 53
- Begelman M.C., Meier D.L. 1982, ApJ 253, 873
- Blandford R.D., Begelman M.C., 1999, MNRAS 303, L17
- Chakravarti S.K., Titarchuk L.G., 1995, ApJ 455, 623
- Chakrabarti S.K., 1996, Phys. Rept. 266, 229
- Chen X., Abramowicz M.A., Lasota J.-P. 1997, ApJ 476, 61
- Chen X., 1995, MNRAS 243, 610
- Fabian A.C., Rees M.J., 1995, MNRAS 277, L55
- Gammie C.F., Popham R., 1998, ApJ 498, 393
- Ichimaru, 1977, ApJ 214, 840
- Kato S., Abramowicz, M.A., Chen X., 1996, MNRAS 278, 236
- Lasota J.-P., Abramowicz M.A., Chen X., et al., 1996, ApJ 462, 142
- Mahadevan R., 1997, ApJ 477, 585
- Narayan R., Yi I., 1994, ApJ 428, L13
- Narayan R., Yi I., 1995a, ApJ 444, 231
- Narayan R., Yi I., 1995b, ApJ 452, 710
- Narayan R., McClintock J.E., Yi. I., 1996, ApJ 457, 821
- Narayan R., Kato S., Honma F., 1997, ApJ 476, 49
- Narayan R., Mahadevan R., Quataert E., 1998, in: Abramowicz M.A., Bjornsson G., J.E. Pringle (eds.), Theory of Black Hole Accretion Disks. Cambridge: Cambridge University Press (astro-ph/9803131)
- Paczynski B., Wiita P.J., 1980, A&A 88, 23
- Peitz J., Appl S., 1997, MNRAS 286, 681
- Rees M.J., Begelman M.C., Blandford R.D., Phinney E.S., 1982, Nat 295, 17
- Spruit H.C., Matsuda T., Inoue M., Sawada K., 1987, MNRAS 229, 517